JAAS

Accepted Manuscript

This is an *Accepted Manuscript*, which has been through the Royal Society of Chemistry peer review process and has been accepted for publication.

Accepted Manuscripts are published online shortly after acceptance, before technical editing, formatting and proof reading. Using this free service, authors can make their results available to the community, in citable form, before we publish the edited article. We will replace this *Accepted Manuscript* with the edited and formatted *Advance Article* as soon as it is available.

You can find more information about *Accepted Manuscripts* in the Information for Authors.

Please note that technical editing may introduce minor changes to the text and/or graphics, which may alter content. The journal's standard Terms & Conditions and the Ethical guidelines still apply. In no event shall the Royal Society of Chemistry be held responsible for any errors or omissions in this *Accepted Manuscript* or any consequences arising from the use of any information it contains.

ROYAL SOCIETY OF CHEMISTRY

www.rsc.org/jaas

Investigation of self-absorption effect in spatially resolved laser-induced breakdown spectroscopy

R.X. Yi, L.B. Guo, C.M. Li , X.Y. Yang, J.M. Li, X.Y. Li *, X.Y. Zeng and Y.F. Lu

Self-absorption effect will seriously influence the accuracy of quantitative analyses in laser-induced breakdown spectroscopy (LIBS). To reduce the self-absorption effect, elements Na, K (major elements) and Pb, Cu (minor elements) in soil plamas have been studied by spatially resolved LIBS (SRLIBS). The 2-dimensions distributions of line intensities and self-absorption coefficients of lines in the plasmas were investigated and the influence parameters of self-absorption effect were also studied. Results have shown that, the self-absorption effect could be reduced greatly and the accuracy of quantitative LIBS could be improved obviously by selecting the collecting zones of the plasmas carefully. Meanwhile, a high laser energy and a short delay time could be useful to expand the region which is influenced slightly by the self-absorption effect.

1. Introduction

As a promising analytical technology, laser-induced breakdown spectroscopy (LIBS) has been widely used in many areas, such as steels,[1-3] ceramics, soil, and water etc.[4-9] With the advantages including fast, real-time, and stand-off analyses,[10-12] LIBS plays an important role in the fields of analytical chemistry. As it's well known, LIBS is based on atomic emission spectroscopy of laser-induced plasma. Due to the complicated laser-matter interactions, the elemental distribution in laser-induced plasmas is often inhomogeneous and some part of the plasma might be optically thick, contained more ground state atoms, which results in the self-absorption effect[13] in LIBS and hence significantly reduce the accuracy of quantitative analyses in LIBS. Therefore, more researchers are working on the ways that can make plasmas uniform and optically thin to avoid self-absorption effect. For instance, Sallé *et al*.[14] studied the *in-situ* LIBS under different atmospheric conditions, and found that the self-absorption effect could be reduced under lower pressure. Some other researchers devoted themselves to solving the problems using data processing methods. For example, Colao *et al*.[15] developed a model by taking into account the effects responsible for non-linearity, and significantly reduced the measured errors caused by the difference of matrix properties, long-term laser instabilities, and self-absorption effect.

These works mentioned above have solved some problems by introducing more experimental setups or utilizing algorithms. Therefore, it is desirable to find a simpler method without introducing more setups to reduce the self-absorption effect. In general, the collecting positions of the spectra from the plasmas are not particularly concerned in LIBS, which might closely influence the intensity and self-absorption effects of the spectra, especially in the inhomogeneous laser-induced plasmas. Therefore, the spatially resolved technique might be a way to obtain higher quality spectra in LIBS. Some research groups have studied the spatially resolved spectra in laser-induced plasmas. For example, Aragon *et al*.[16] studied 2-D spatial distribution of spectra in laser-induced plasmas. Cristoforetti *et al*.[17] studied the morphology of plasmas excited by single and double laser pulses. Meanwhile, the spatial distributions of plasma temperature, electron density, and spectral intensity were used to better understand the plume evolution and physical processes. Chen *et al*.[18] used spatially resolved laser-induced breakdown spectroscopy (SRLIBS) to detect aluminum and silicon elements. Yu *et al*.[19-21] carried out a series of experiments to study the spectral spatial distributions of organic samples in Ar atmosphere, and found that spectral intensity distributions varied from element to element.

Research works described above had achieved good results about intensity distributions of spectra corresponding to different collecting positions of laser-induced plasmas, but few works focused on the self-absorption effects in the plasmas. In this work, the SRLIBS technique has been used to study the relationship between self-absorption effect and collection positions.

2. Experimental setup and method

The schematic experimental setup is shown in Figure 1(a). A Q-switched Nd: YAG laser (wavelength: 532 nm, repetition rates: 10 Hz, pulse width: 6 ns, pulse energy: 20 mJ) was focused by a plano-convex lens (f = 150 mm) with a focal point at 2 mm below the soil surface to generate plasmas in air. Two lenses (f = 100 mm) were used to project the plasma emission to the image plane. An optical fiber (core diameter: 50 μm) clamped by a triaxial holder (positioning accuracy: 1 μm) was placed in the image plane to collect spectra of the plasma at specific positions. The spectra were collected by an echelle spectrometer (Andor Tech., Mechelle 5000, wavelength range: 240-880 nm, spectral resolution: $\lambda/\Delta\lambda$ = 5000) equipped with an intensified charge-coupled device (ICCD) (Andor Tech., iStar 334T). A digital delay generator (Stanford Research Systems, DG535) was employed to trigger the laser pulses and control the gate delays and widths of the ICCD. The spectra were collected at a delay time of 4 μs and gate width of 2 μs. The samples were mounted onto a motorized XYZ translation stage and were moved in a straight line to provide a fresh surface for each laser pulse. The distance between two collecting positions in the image plane of plasma is 100 μm, with a whole collecting area of 1200×1200 μm^2. To reduce the standard deviation of spectral intensities, each spectrum was accumulated for 50 pulses. 10 spectra was taken and averaged at each position of the plasma.

Two kinds of soil samples approved by the State Administration of Quality Supervision, Inspection, and Quarantine of China were used in this work. They were GBW070008 and GBW07407, respectively. GBW070008 was used to investigate self-absorption effect in soil plasma, due to its high concentration of K element, as shown in table 1. GBW07407 was used to analyse the K

elements quantitatively, due to its low concentration of K element (the original K concentration is 0.16%, by adding KCl in the soil samples, a broader scope of K concentration could be obtained), and 7 new samples were prepared through adding KCl into the GBW07407. The concentrations of K element in the prepared samples were shown in table 2. The soil powder samples were pressed into pellets with a diameter of 2 cm under a pressure of 20 MPa as shown in Fig. 1(b).

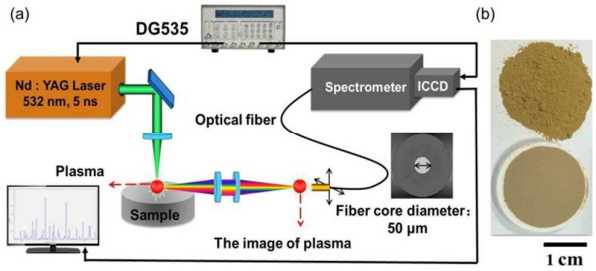

Fig. 1 The experimental setup (a) and the sample (b).

Table 1. The concentrations of different elements in GBW070008.

Element	Na	K	Pb	Cu
Concentration (ppm)	14800	26700	675	290

Table 2. The concentrations of K element in the prepared samples.

No.	1	2	3	4	5	6	7
Con. (%)	0.16	0.5	1	2	3	4	5

3. Results and discussion

The coordinate system of the spatial distributions of plasmas from the soil samples is defined as Figure 2. The origin is at the center of the plasma. The laser is incident from the Z axis. The optical emission detection is along with the Y axis. The (X, Z) coordinates represent the detection position.

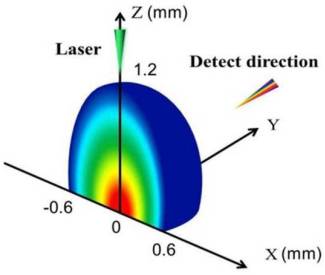

Fig. 2 The self-defined coordinate system for the plasma.

To minimize the influence of the continuous spectrum and obtain strong intensity, the spectra were collected at an optimized delay time of 4 μs and gate width of 2 μs.

3.1 Spectral intensity distributions

Spectral intensity is very important in LIBS. To study the spectral intensity distributions of major and minor elements in soil plasmas, 2D distributions of the spectral intensity were obtained.

Figure 3 shows the spectral intensity distributions of the major elements (e.g., Fig. 3(a) Na I 589.7 nm and Fig. 3(b) K I 769.9 nm) and the minor elements (e.g., Fig. 5(c) Pb I 405.8 nm and Fig. 3(d) Cu I 327.4 nm) in the soil plasmas. As shown in Figs. 3(a)-3(d), the main difference between the spectral intensities of the minor and major elements appears in the upper part of the plasma (area surrounded by the pink dashed circles). The spectral intensities (peak above baseline) of both Na I 589.7 nm and K I 769.9 nm decrease significantly in this area, whilst the spectral intensities of both Pb I 405.8 nm and Cu I 327.4 nm maintain high in the same area, which shows that the spectral intensities of different elements distribute differently. Similar results were also obtained by Yu *et al*. [19] for pure aluminum samples in an argon ambient gas under one atmosphere pressure.

Generally, the spectra near the central part maintain high intensity, and decrease slowly from the central part to the periphery of the plasma for Pb and Cu elements. However, for Na and K elements, a special phenomenon appears, the spectra in the upper part of the plasma decrease rapidly. This difference will be explained in the section below.

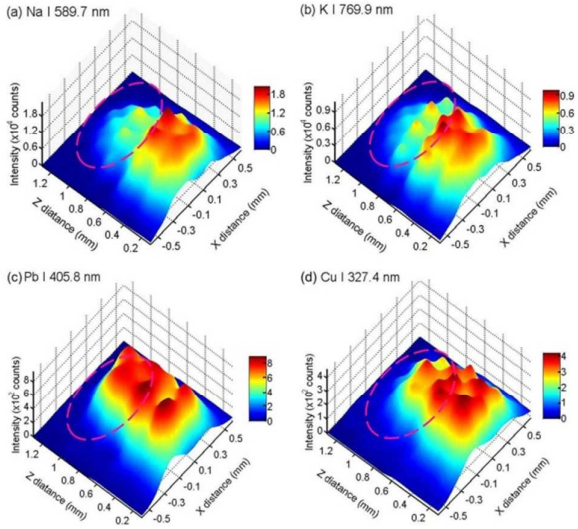

Fig. 3 Spectral intensity distributions of the major elements Na (Na I 589.7 nm) (a), K (K I 769.9 nm) (b), and the minor elements Pb (Pb I 405.8 nm) (c), Cu (Cu I 327.4 nm) (d) in soil plasmas. The pink circles represent the area where marked the differences between the minor elements and the major elements.

3.2 Self-absorption distributions

Apart from the spectral intensity, the self-absorption effect is also significant in LIBS. Figures 4(a)-4(d) show the spectra of the Na, K, Pb, and Cu elements that were collected at two typical positions [(0, 0.7) and (0, 0.2)] of soil plasma. It could be found that, the spectral intensity at the position (0, 0.2) are higher than those at the position (0, 0.7), especially for Na and K element. Meanwhile, serious self-absorption effects of Na and K element are observed at the position (0, 0.7), which causes the rapid decreasing of the spectral intensity. However, for Pb and Cu elements, the spectra of

them are influenced slightly by the self-absorption effect, due to the "normal" shape of the spectra and the lower concentration of the elements[22, 23].

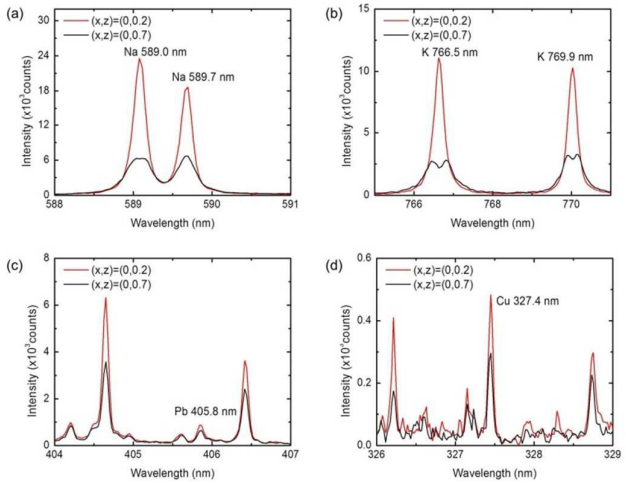

Fig. 4 The spectra of Na I 589.0 nm, Na I 589.7 nm (a), K I 766.5 nm, K I 769.9 nm (b), Pb I 405.8 nm (c), and Cu I 327.4 nm (d) in the soil plasmas. The red lines denote the spectra at the detection position of (0, 0.2) and the black lines denote the spectra at the detection position of (0, 0.7).

To study the self-absorption distributions of the plasma, a coefficient was used to represent the degree of self-absorption effect. Cristoforetti *et al.* [24] deduced Eq. (1) to calculate the coefficient, which was named as SA,

$$SA = \left(\frac{\Delta\lambda}{\Delta\lambda_0}\right)^{\frac{1}{\alpha}}, \quad (1)$$

where $\Delta\lambda$ is the full width at half maximum (FWHM) of the observed line, $\Delta\lambda_0$ is the FWHM of the line without the self-absorption effect, and α is a constant. Among these parameters, $\Delta\lambda_0$ can only be calculated by Eq.(2),

$$\Delta\lambda_0 = 2\omega_{s0} n_e, \quad (2)$$

where n_e is the electron density, ω_{s0} is the half-width Stark parameter the element. As it is time-consuming and tedious to calculate n_e and obtain ω_{s0}, to simplify the calculative process, Eq. (1) is equivalent to

$$SA = \left(\frac{\Delta\lambda}{\Delta\lambda_0}\right)^{\frac{1}{\alpha}} = \left(\frac{\Delta\lambda}{\Delta\lambda_a} \bullet \frac{\Delta\lambda_a}{\Delta\lambda_0}\right)^{\frac{1}{\alpha}} = \left(\frac{\Delta\lambda}{\Delta\lambda_a} \bullet \frac{n_e\omega_{sa}}{n_e\omega_{s0}}\right)^{\frac{1}{\alpha}}, \quad (3)$$

where, $\Delta\lambda_a$ is the FWHM of another line without the self-absorption effect, ω_{sa} is the half-width Stark parameter the element, and ω_{s0}/ω_{sa} is a constant. SA represents the degree of the self-absorption effect quantitatively, however, what needed in this part is just the changing trend of the self-absorption effect, so parameter k was assumed to represent the changing trend of self-absorption effect,

$$k = SA^{\alpha} \bullet \frac{\omega_{s0}}{\omega_{sa}} = \frac{\Delta\lambda}{\Delta\lambda_a}. \quad (4)$$

As the shape of Fe I line at 440.5 nm is normal and the lower level of it is 12560.934 cm^{-1}, which is much higher than the ground state level. This line is considered less affected by the self-absorption effect in the soil plasma. Therefore, it was chosen to calculate $\Delta\lambda_a$.

Figures 5(a) and 5(b) show the self-absorption coefficient distributions of both Na I 589.0 nm and K I 769.9 nm in the XZ plane by calculating k using Eq. (4). It is found that, the k in the areas of Z < 0.6 mm remains very low, whilst k in the areas of Z >= 0.6 mm increases rapidly as increasing Z for both elements. The RSDs of k in the whole XZ plane are 40.4% and 67.0% for Na and K elements, respectively. These results suggest that the self-absorption effect in the upper part of the plasma is much more serious than that in the lower part of the plasma. The self-absorption effects at different positions of the plasma are different for the major elements. Assuming that the plasma has a hemispherical shape, it can be said that the temperature field also takes a spherical symmetry in the half space, hotter inside and colder outside. In this case, when the detection plane moves along the z direction from the sample surface, the ratio of hot plasma volume to cold plasma volume drops rapidly, which results in the differences. However, as shown in Figs. 5(c) and 5(d), the self-absorption coefficients of the minor elements remain very low in the whole plasma region (the blue region). Moreover, the RSDs of k in the whole XZ plane are only 5.4% and 4.7% for both Pb and Cu elements, respectively. These results suggest that the self-absorption is not serious for the minor elements in the whole plasma region.

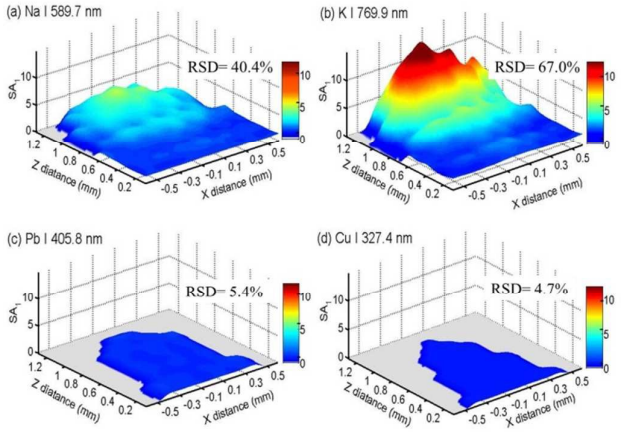

Fig. 5 Self-absorption coefficient distributions of the major elements Na (Na I 589.7 nm) (a), K (K I 769.9 nm) (b), and the minor elements Pb (Pb I 405.8 nm) (c), Cu (Cu I 327.4 nm) (d) in the XZ plane. RSDs of k in the whole plasma plane were 40.4%, 67.0%, 5.4%, and 4.7% for Na I 589.7 nm, K I 769.9 nm, Pb I 405.8 nm, and Cu I 327.4 nm, respectively.

3.3 Temperature and ground state atoms distributions

Plasma temperature is an important parameter for laser-induced plasma. Obtaining the spatial distribution of plasma temperature would benefit the further understanding of the relationship between the temperature and the self-absorption effect of the plasma. Moreover, because the self-absorption effect is related to the number of ground state atoms, the number of ground state atoms was also studied in this section.

The temperature is calculated by Boltzmann plot and 14 titanium (Ti) lines I were chosen for plotting, as shown in Table 3. As

the distribution difference of self-absorption effect mainly changed along the Z axis of the plasma, the temperature is only calculated along the Z axis of the plasma. Figure 6 shows the temperature distribution of the plasma, the temperature increases from Z= 0 mm to Z= 0.3 mm, then it decreases rapidly from Z= 0.3 mm to Z= 0.9 mm. Because the spectra are too weak to calculate the temperature when Z> 1 mm, the temperature are only calculated from Z= 0 mm to Z= 0.9 mm.

Table 3. The spectral information of Ti I.

λ (nm)	E(ev)	A(×10^7)	g	λ (nm)	E(ev)	A(×10^7)	g
363.55	3.41	9.09	7	454.47	3.55	3.30	3
364.27	3.42	8.95	9	461.73	4.43	8.51	9
365.35	3.44	8.69	11	462.31	4.42	5.74	7
375.29	3.35	5.81	9	468.19	2.70	2.71	11
398.18	3.11	4.42	5	500.72	3.29	4.92	7
398.98	3.13	4.48	7	506.47	2.50	4.37	7
399.86	3.15	4.81	9	521.04	2.43	3.89	9

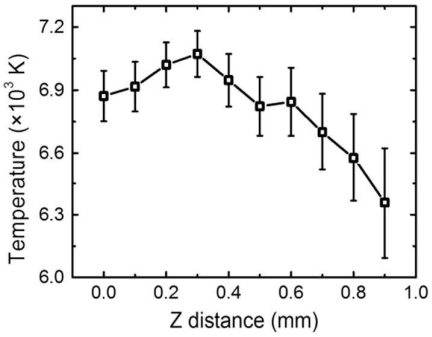

Fig. 6 Plasma temperatures along Z axis

The ratios of the number of ground state atoms and the number of total atoms can be obtained by the following equation:

$$\frac{n_0^s}{n} = \frac{g_0 \cdot n_s}{n \cdot U^s(T)} e^{-E_0/kT}, \quad (5)$$

where n_0^s is the number of particles which locate at energy level 0, g_0 and E_0 represent the degeneracy and energy of level 0, n^s represents the number of element s in the plasma, n represents the number of all the atoms in the plasma.

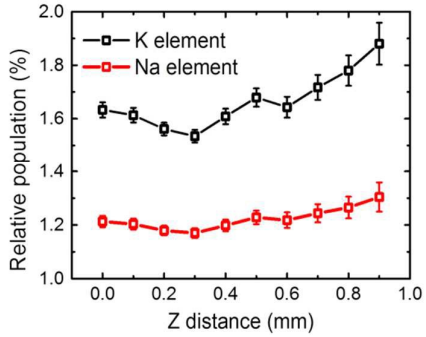

Fig. 7 Relative population of K and Na atoms on ground state at different positions on Z axis.

Figure 7 shows the n_0^s/ n of Na and K elements along the Z axis. The relative population of ground state atoms for K and Na elements decreases from Z= 0 mm to Z= 0.3 mm, then it increases rapidly from Z= 0.3 mm to Z= 0.9 mm, and the relative population of ground state atoms of K element is larger than that of Na element, which will result in more serious self-absorption effect for K element. Furthermore, the self-absorption effects of Na and K elements are more serious at the locations of high n_0^s/ n value and high temperature (e.g., Z>=0.6 mm), as shown in Figs. 5 and 6. Therefore, it can be conclude that, the self-absorption distribution is closely related to the plasma temperature and the relative population of ground state atoms for Na and K elements.

3.4 Influences of laser energy, delay time and element concentration on the self-absorption effect

The above results show that, the self-absorption effect distributes differently in the whole plasma region, and an obvious boundary can be used to divide the plasma into two parts. Because the distribution difference of self-absorption effect mainly changed along the Z axis, the critical Z position where the self-absorption effects would appear is defined as the first self-reversal point. By using the first self-reversal point, the plasma could be divided into two parts effectively. As shown in Figure 8, the spectra acquired below Z = 0.6 mm (white region) are influenced slightly by the self-absorption effect, but the spectra at Z > 0.6 mm (red region) are affected by the self-absorption effect seriously. Therefore, Z= 0.6 mm is the first self-reversal point in the certain conditions. In concrete, 10 spectra were acquired in each acquisition position and experimental parameter, the position could be regarded as the first self-reversal point, when more than 5 spectra (acquired at this position) appeared self-reversal.

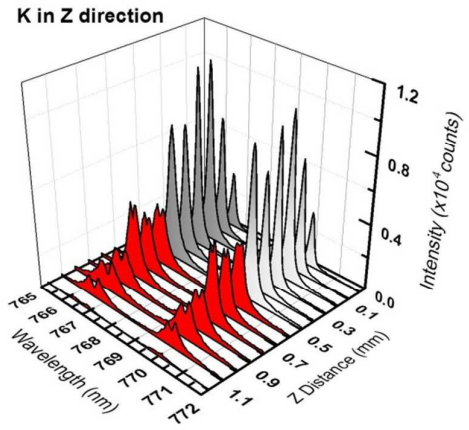

Fig. 8 Spectra of K I 769.9 nm from Z= 0 to Z=1.2. The laser energy was 20 mJ, the delay time was 4 μs, the gate width was 2 μs, and the K concentration is 2.67%.

Figures 9, 10 and 11 show the influences of laser energy, delay time and K concentration on the first self-reversal points of K I 769.9 nm, respectively. Fig. 9 shows the effect of laser energy on the first self-reversal point, the first self-reversal point rises from 0.3 to 1.6 mm as the laser energy increases from 10 to 80 mJ. In Fig. 10, the delay time began from 1 μs, and the step was 1 μs, as well. The laser energy was 20 mJ, the acquisition position was set from 0

to 1.0 mm. The first self-reversal point drops from 0.7 to 0.4 mm as the delay time increases from 1 to 10 μs. Fig. 11 shows the effect of concentration. The first self-reversal point of K I 769.9 nm drops from 1.5 mm to 0.2 mm as the K concentration increases from 0.16% to 5%.

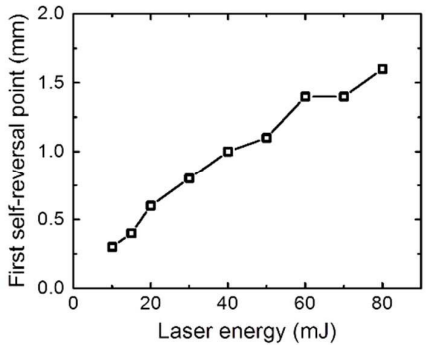

Fig. 9 Influence of laser energy on the first self-reversal point of K I 769.9 nm in the plasma. The delay time was 4 μs and the gate width was 2 μs.

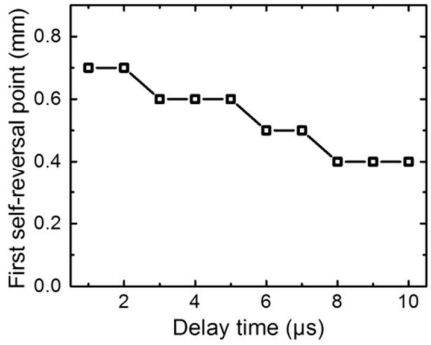

Fig. 10 Influence of delay time on the first self-reversal point of K I at the 769.9 nm in the plasma. The laser energy was 20 mJ and the gate width was 1 μs.

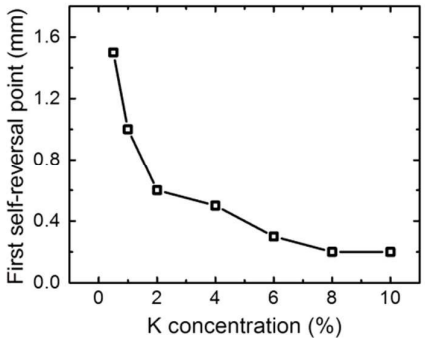

Fig. 11 Influence of K concentration on the first self-reversal point of K I 769.9 nm in the plasma. The laser energy was 20 mJ, the delay time was 4 μs and the gate width was 2 μs.

Figures 9 and 10 show that, the larger laser energy and the shorter delay time are, the higher first self-reversal point in the plasma will be. Because the plasma temperature is higher with larger laser energy and shorter delay time[25, 26], the results show that, there is a positive relationship between the plasma temperature and the height of the first self-reversal point. Figure 11 shows the negative relationship between the element concentration and the height of the first self-reversal point. It was demonstrated experimentally that, the distribution of self-absorption effect in the plasma is affected by the plasma temperature (determined by laser energy and delay time) and the concentration of the element.

3.5 Influence of collecting position on quantitative analysis of potassium

To study the Influence of collecting position on quantitative analysis of potassium, three typical positions were chosen to analyze the K element quantitatively. Z= 0.1 mm represents the lower part of the plasma, Z= 0.6 mm represents the first self-reversal point of the plasma and Z= 1 mm represents the upper part of the plasma.

Figure 12(a) shows calibration curves (linear fitting) obtained on K I 769.9 nm at the typical positions Z= 0.1 mm, Z= 0.6 mm and Z= 1.0 mm in soil plasmas. The R-Squares (linear fitting) obtained at the three typical positions are 0.9891, 0.8317 and 0.8369, respectively. Figure 12(b) shows the enlarged calibration curves (quadratic fitting) at the positions Z= 0.6 mm and Z= 1.0 mm in soil plasmas. The R-Squares (quadratic fitting) obtained at the positions are 0.9668 and 0.9699, respectively. Due to the self-absorption effect, the peak intensity of K I 769.9 nm (No. 5, 6, 7 with a high concentration) at the detection positions of Z=0.6 mm (red line) and Z=1.0 mm (blue line) decrease. Meanwhile, the R^2 obtained at Z=0.1 mm is much better than those at Z=0.6 mm and Z=1.0 mm in the plasma, due to low self-absorption effect at these detection positions. Furthermore, the averaged RSD for the 7 samples at the detection positions of Z=0.1 mm, Z=0.6 mm and Z=1.0 mm are 9.2%, 22.9% and 58.3%, respectively, which means that the signals become more unstable due to the serious self-absorption effect in the upper part of the plasma. These results show that, the self-absorption effect of the major elements can be reduced effectively by selecting different positions using SRIBS.

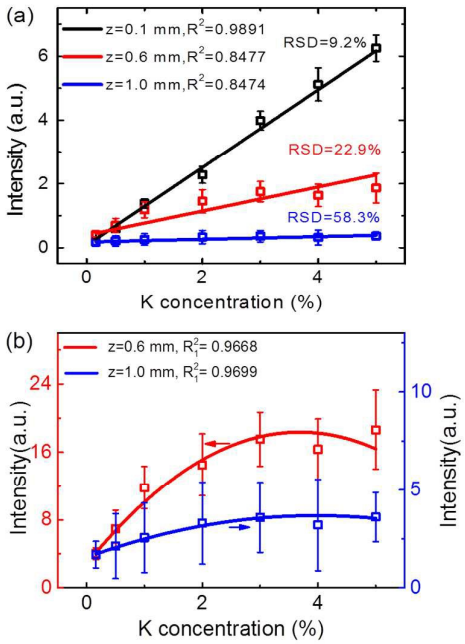

Fig. 12 The calibration curves (linear fitting) of K I 769.9 nm at the detection positions of Z= 0.1 mm (black line), Z = 0.6 mm (red line) and Z = 1.0 mm

(blue line) (a), the enlarged calibration curves (quadratic fitting) at the positions Z= 0.6 mm and Z= 1.0 mm (b).

3.6 Self-absorption distributions in other matrices

To investigate whether the self-absorption effect distribute differently in other matrices, a simplified experiment was carried out. Self-absorption distributions in the plasma of other matrices ($CaCl_2$ and pure Al) were studied. The first self-reversal point exists in these matrices as well. As shown in Figure 13, spectra of Ca I 422.7 nm and Al I 309.3 nm were obtained from Z = 0 mm to Z = 1.1 mm, and the first self-reversal points are Z = 0.6 mm and Z = 0.3 mm for Ca and Al, respectively. The results show that, the inhomogeneous distribution of self-absorption effect exists in not only soil matrix, but also other matrix as well.

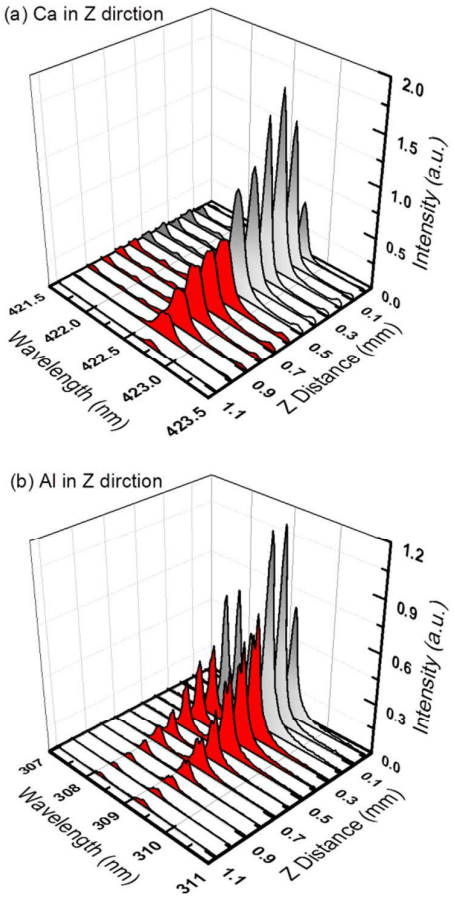

Fig. 13 Spectra of Ca I 422.7 nm (a) and Al I 309.3 nm (b) obtained from Z =0 to Z =1.1. The laser energy was 20 mJ, the delay time was 4 μs and the gate width was 2 μs.

4. Conclusion

The spatial distributions of spectral intensity and self-absorption of laser-induced soil plasmas were investigated. The results show that the characteristics of the LIBS spectra have inhomogeneous distribution at different positions in the plasmas. By analyzing Na, K, Pb, and Cu elements, the distributional differences for both major and minor elements have been studied. The influence of laser energy, delay time and element concentration on the self-absorption effect has been studied as well. The results show a close relationship between the distribution of self-absorption effect and these parameters. Furthermore, for the major elements, spectra with higher intensity and lower self-absorption could be obtained when the collecting position is at the lower part of the plasmas. The results of quantitative analysis for potassium through SRLIBS show that, the self-absorption effect of the major element can be reduced effectively by selecting different positions using SRIBS. Meanwhile, the similar phenomenon has been observed in other matrix (Al and $CaCl_2$), which shows that this technique can be applied in other materials as well.

Acknowledgments

This research was financially supported by the Major Scientific Instrument and Equipment Development Special Funds of China (No. 2011YQ160017), the National Natural Science Foundation of China (No. 61575073, 51429501 and 61378031), and the Fundamental Research Funds for the Central Universities (HUST: 2015TS075).

Notes and References

Wuhan National Laboratory for Optoelectronics (WNLO), HuaZhong University of Science and Technology, Wuhan, Hubei 430074, PR China. Fax: 86-27-87541423; Tel: 86-27-87541423; E-mail: xyli@mail.hust.edu.cn

References and links

1. D. W. Hahn and N. Omenetto, *Appl. Spectrosc*，2010, **64**, 335A-366A.
2. R. Noll, Laser-induced breakdown spectroscopy, *Springer,* 2012.
3. Z. Hao, L. Guo, C. Li, M. Shen, X. Zou, X. Li, Y. Lu and X. Zeng, *J. Anal. At. Spe*ctrom., 2014, 29, 2309-2314.
4. J. P. Singh and S. N. Thakur, Laser-induced breakdown spectroscopy, Elsevier, 2007.
5. Z. Wang, T.B. Yuan, Z.Y. Hou, W.D. Zhou, J.D. Lu, H.B. Ding, and X.Y. Zeng, Front. Phys. 2014, 9(4): 419-438
6. L. B. Guo, Z. Q. Hao, M. Shen, W. Xiong, X. N. He, Z. Q. Xie, M. Gao, X. Y. Li, X. Y. Zeng, and Y. F. Lu, *Opt. Express,* 2013, **21**, 18188-18195.
7. A. M. Popov, F. Colao and R. Fantoni, *J. Anal. At. Spectrom.*, 2010, **25**, 837-848.
8. A. Pal, R. D. Waterbury, E. L. Dottery, and D. K. Killinger, *Opt. Express*, 2009, **17**, 8856-8870.
9. M. H. Ebinger, M. L. Norfleet, D. D. Breshears, D. A. Cremers, M. J. Ferris, P. J. Unkefer, M. S. Lamb, K. L. Goddard, and C. W. Meyer. *Soil Sci. Soc. Am. J.*, 2003, **67**, 1616-1619.
10. J.D. Winefordner, I.B. Gornushkin, T. Correll, E. Gibb, B.W. Smith and N. Omenetto, *J. Anal. At. Spectrom.*, 2004, **19**, 1061-1083.
11. M. J. C. Pontes, J. Cortez, R. K. H. Galvão, and C. Pasquini, *Anal. Chim. Acta*, 2009, **642**, 12-18.
12. J. Pareja, S. López, D. Jaramillo, D. W. Hahn, and A. Molina, *Appl. Opt.*, 2013, **52**, 2470-2477.
13. D. A Rusak, B. C Castle, B. W Smith, and J. D Winefordner, *Trac-Trend Anal. Chem.*, 1998, **17**, 453-461.
14. B. Sallé, D.A. Cremers, S. Maurice, and R. C. Wiens, *Spectrochim. Acta Part B,* 2005, **60**, 479-490.
15. V. Lazic, R. Barbini, F. Colao, R. Fantoni, and A. Palucci, *Spectrochim. Acta Part B,* 2001, **56**, 807-820.
16. C. Aragon and J. A. Aguilera, *Appl. Spectrosc.,* 1997, **51**, 1632-1638.
17. M. Corsi, G. Cristoforetti, M. Giuffrida, M. Hidalgo, S. Legnaioli, V. Palleschi, A. Salvetti, E. Tognoni, and C. Vallebona, *Spectrochim. Acta Part B,* 2004, **59**, 723-735.
18. S. J. J. Tsai, S. Y. Chen, Y. S. Chung, and P. C. Tseng, *Anal. Chem.*, 2006, **78**, 7432-7439.

19. J. Xiu, X. Bai, E. Negre, V. M. Ros, and J. Yu, *Appl. Phys. Lett.*, 2013, **102**, 244101-1-6.
20. X. Bai, Q. Ma, V. M. Ros, J. Yu, D. Sabourdy, L. Nguyen, and A. Jalocha, J. *Appl. Phys.*, 2013, **113**, 013304-1-10.
21. J. Yu, Q. Ma, V.M. Ros, W. Lei, X. Wang, and X. Bai, *Front. Phys.*, 2012, **7**, 649-669.
22. V.K. Unnikrishnan, R. Nayak, K. Aithal, V.B. Kartha, C. Santhosh, G.P. Guptac and B.M. Suric, Anal. Methods, 2013, **5**, 1294-1300.
23. S. Pandhija, A.K. Rai. Environmental monitoring and assessment, 2009, 148, 437-447.
24. A.M.E. Sherbini, T.M.E Sherbini, H. Hegazy, G. Cristoforetti, S. Legnaioli, V. Palleschi, L. Pardini, A. Salvetti, and E. Tognoni, *Spectrochim. Acta Part B,* 2005, **60**, 1573-1579.
25. O. Barthélemy, J. Margot, M. Chaker, M. Sabsabi, F. Vidal, T. Johnston, S.Laville, B. L. Drogoff, *Spectrochim. Acta Part B,* 2005, **60**, 905-914.
26. S. Laville, F. Vidal, T. Johnston, M. Chaker, B.L. Drogoff, O. Barthelemy, J. Margot, M. Sabsabi, *Physics of Plasmas* (1994-present) 2004, **11**, 2182-2190.